

MARCI GLOBAL DAILY OZONE MAPPING AND COMPARISON TO LMDGCM SIMULATIONS: POLAR DYNAMICS, HELLAS BASIN, AND HETEROGEOUS CHEMISTRY

R. T. Clancy, M. J. Wolff, *SSI, Boulder, CO, USA (clancy@spacescience.org)*, F. Lefèvre, F. Forget, *LATMOS, Paris, France*, M. Malin, *MSSS, San Diego USA*, and M. D. Smith, *GSFC, Greenbelt, MD, USA*.

Introduction:

The Mars Color Imager (MARCI) on Mars Reconnaissance Orbiter (MRO) has obtained daily global image maps of Mars in two UV filters since 2006 (figure 1), supporting Hartley band mapping retrievals for Mars atmospheric O₃ columns^{1,2}.

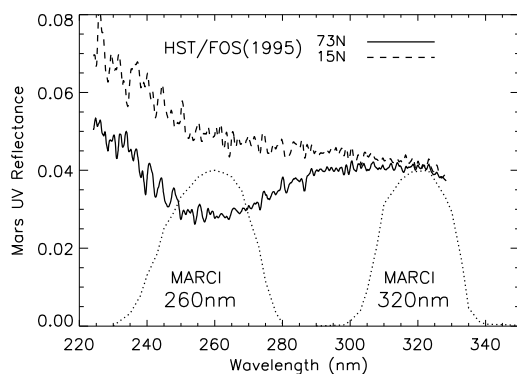


Figure 1. MARCI two UV bandpasses presented against Hubble Space Telescope spectra of Mars O₃¹.

Here, we present three specific subsets of this extensive ($\sim 10^{10}$) measurement set, in comparison with Laboratoire de Météorologie Dynamique (LMD) Global Climate Model (GCM) simulations of Mars photochemistry^{3,4}. We focus on aspects of the MARCI O₃ data set pertaining to polar dynamics, striking seasonal variations within Hellas basin, and the possibility of heterogeneous chemistry on Mars clouds⁴. In the context of these comparisons, we include MARCI cloud optical depth⁵ and SPICAM O₃ column⁶ measurements.

Polar Dynamics:

Mars atmospheric odd-oxygen, of which O₃ is the primary daytime constituent, is rapidly destroyed by odd-hydrogen products of daytime water vapor dissociation^{7,8}. This enforces a well established inverse relationship between Mars atmospheric O₃ and water vapor^{9,10}. In particular, maximum O₃ columns (10-50 $\mu\text{m-atm}$) are presented at Mars high latitudes in colder seasons (late fall, winter, early spring) when atmospheric water columns fall below 1 $\text{pr-}\mu\text{m}$ ^{3,6,9}. As MARCI retrieval sensitivity ($>1 \mu\text{m-atm}$) limits low latitude O₃ measurements to the aphelion season^{2,6} and the polar MRO orbit maximizes daily image coverage at high latitudes, cold (non-summer) polar regions provide optimal occurrence and resolution of O₃ spatial and seasonal variations. To first

order, these variations are driven by planetary wave deformation of sharp latitudinal gradients in O₃ columns associated with the polar vortex boundary to the cold, isolated polar air mass³. Consequently, MARCI daily polar imaging of polar O₃ variations supports a spatially contiguous, well-resolved ($\sim 10\text{km}$) definition of polar wave activity on a daily basis over portions of 5 Mars years (MY28-32, and counting).

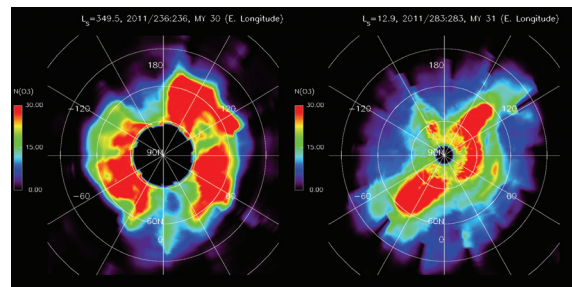


Figure 2. Two MARCI north polar O₃ maps obtained in northern early spring ($L_s=350^\circ$ and 13° , MY30/31) display wavenumber 3 and 2 planetary wave structures².

In figure 2, we present a pair of MARCI polar projected maps indicating the degree and variable character to which such waves are displayed in MARCI O₃ column measurements. The contoured O₃ columns exhibit polar distributions associated with wavenumber 3 and 2 distortions of the polarvortex boundary.

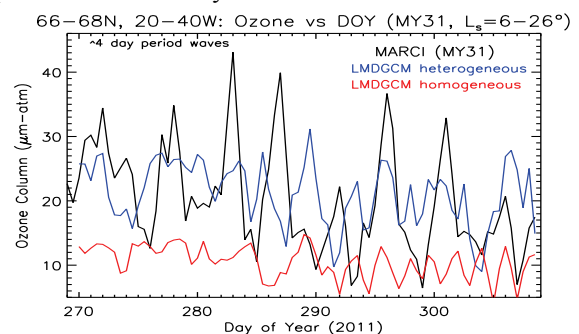


Figure 3. Observed (black) and modeled (color) periodic variations in high-latitude O₃ columns (northern spring)².

In figure 3, we plot the variation of O₃ at 66-68N, 20-40W over $L_s=6-26^\circ$ (MY31), in which a ~ 4 -day period of planetary wave activity is apparent the MARCI observations (solid black line), and to a varying degree in LMD GCM simulations with (blue line) and without (red line) heterogeneous chemistry.

The observed variability in high latitude O₃ abundance contributes partly to the argument for heterogeneous chemistry on clouds⁴, as discussed later in this abstract.

Hellas Seasonal O₃ Variation:

Hellas basin presents significantly increased surface pressures, up to several times those exhibited by much of the elevated southern hemisphere of Mars.

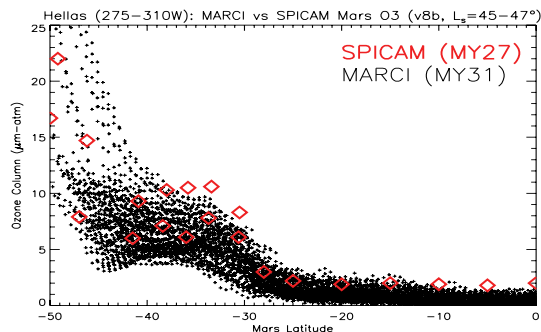


Figure 4. The latitudinal distribution of Mars O₃ over Hellas longitudes during southern late spring. Increased O₃ in MARCI (black) and SPICAM (red) measurements appears at the southern edge of Hellas.

As O₃ is formed by three-body reaction including CO₂, Hellas O₃ abundances are generally enhanced. Figure 4 presents a latitude cross-section of MARCI² and SPICAM⁶ O₃ column measurements over the Hellas basin longitudes, demonstrating this effect as well as the general agreement between MARCI and SPICAM O₃ retrievals.

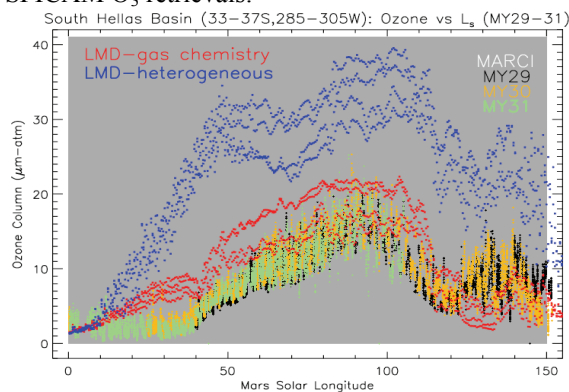


Figure 5. The fall-to-winter seasonal behavior of Hellas basin O₃ columns is presented for MY29-31 MARCI measurements and LMD GCM simulations².

Figure 5 presents the seasonal (L_s) variation of O₃ within Hellas (specifically, 33-37S and 285-305W), as measured by MARCI over MY29-31 (black, yellow, green) and simulated by the LMD GCM with (blue) and without (red) heterogeneous chemistry on clouds. Minimal O₃ inter-annual variation is apparent in the MARCI measurements. Two distinct seasonal peaks in Hellas O₃ are centered at L_s of 90° and 135° in the observations and models (and a third peak in the heterogeneous chemistry model at 55°). The sharp decrease in Hellas O₃ after $L_s \sim 100^\circ$ extends into the northern hemisphere and

reflects a seasonal/orbital transition in the distribution of upper level (above 10-20 km) atmospheric water vapor distribution.

The second seasonal peak over $L_s = 130-150^\circ$ may reflect additional seasonal variation in atmospheric water vapor over Hellas at this time¹¹. However, CRISM water vapor column retrievals¹² over non-Hellas basin longitudes (but the same latitudes) present monotonic increases after $L_s = 100^\circ$. Furthermore, MARCI O₃ columns at non-Hellas longitudes do not show such an $L_s = 130-140^\circ$ peak, whereas they do exhibit O₃ decreases after $L_s = 90^\circ$ similar to Hellas O₃ behavior at this time. Alternatively, it is possible that polar condensation enrichment processes are related to this Hellas basin O₃ increase. For example, condensation-enriched O₃ from winter polar regions may be transported into the deep Hellas basin as the southern polar vortex begins to weaken with the advancing southern spring season.

Two Hellas basin CO mixing ratio retrievals from MEX OMEGA $L_s = 132-140^\circ$ observations exhibited 50-100% increases relative to other observed L_s periods, and to northern latitudes in the same season¹³. This behavior was also reflected in LMD GCM simulations and attributed to condensation enrichment of CO at winter high latitudes¹⁴. MRO CRISM CO mixing ratio measurements¹² over Hellas basin (lower panel in figure 6) also exhibit significant L_s variations relative to other longitudes (top panel in figure 6, noisier due to lower surface pressures), with peak values over $L_s = 150-160^\circ$. However, there is a significant gap in CRISM CO (and H₂O) observations over $L_s = 80-150^\circ$ that limits clear comparisons to the MARCI O₃ (or OMEGA CO) variations. We are planning new CRISM measurements for coverage in this season.

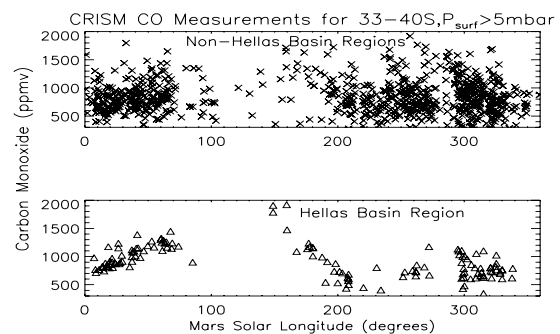


Figure 6. The seasonal (L_s) dependence of CO mixing ratios outside (top panel) and within (bottom panel) Hellas basin, for 33-40S latitudes and surface pressures > 5 mbar.

Of course, the LMD GCM simulates the key processes and reproduces the observed Hellas O₃ (and possibly CRISM CO) variations reasonably well. This suggests good constraints may soon be placed the specific atmospheric processes that lead to the observed Hellas O₃, H₂O, and CO variations.

Heterogeneous Chemistry on Clouds:

The role of heterogeneous chemistry on Mars clouds in removing HO_x (thus increasing O_3) has been proposed to account for LMD GCM model disagreements with O_3 and H_2O_2 measurements⁴. Comparisons of MARCI to LMD GCM O_3 columns show improvement with heterogeneous chemistry in some cases (figure 3), but substantially reduced agreement in other cases (figure 5). This variable level of agreement between MARCI and model O_3 columns, associated with implementation of heterogeneous chemistry, is further displayed in figure 7. In this case, observed and modeled O_3 columns at 70-74N are plotted over $L_s=0-100^\circ$, encompassing the seasonal decrease high latitude O_3 from northern early spring to summer. Heterogeneous chemistry on clouds (blue) leads to larger O_3 abundances in early spring, in accordance with the MARCI observations (black). However, these enhanced model O_3 columns persist later in season ($L_s=60^\circ$) than indicated by the MARCI observations ($L_s=30^\circ$).

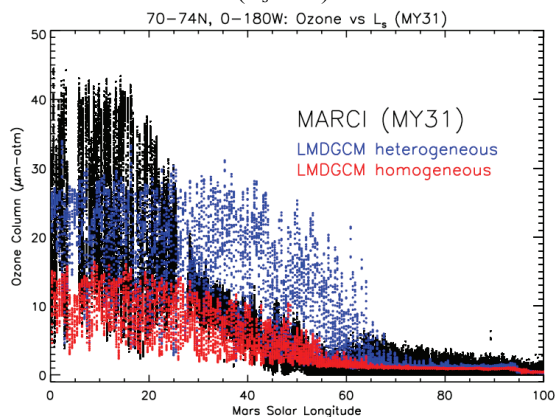


Figure 7. The seasonal dependence of Mars O_3 columns over 70-74N and 0-180W longitudes as observed (black-MARCI) and modeled (LMD GCM, blue-heterogeneous versus red-homogeneous chemistry).

MARCI measurements also support cloud optical depth retrievals ($\lambda \sim 320$ nm) coincidentally with the column O_3 measurements⁵. However, MARCI cloud measurements are valid only over non-surface-ice regions. Under this restriction, we have searched for possible correlations in MARCI cloud and O_3 measurements. In figure 8, we plot northern fall ($L_s=180-200^\circ$) MARCI O_3 column versus cloud optical depth measurements for 66-68N (all longitudes). No obvious correlation is presented between cloud and O_3 MARCI measurements at this time.

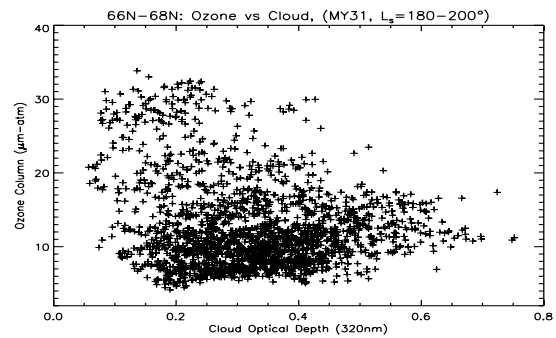


Figure 8. MARCI O_3 column and cloud optical depth measurements do not exhibit a notable correlation at high northern fall latitudes in MY31.

In figure 9, we compare MARCI observed ~ 5 day variations in southern fall O_3 columns (top panel) over a limited region (48-52S, 130-160W) with coincident cloud optical depth variations (bottom panel). As indicated by vertical yellow bars, dates of peak O_3 columns do not correspond to peak cloud optical depths. For both figures 7 and 8, the observed O_3 variations are dominated by large-scale waves in the presence of strong latitudinal gradients for O_3 columns. We point out that no clear correlation is present between MARCI cloud and O_3 abundances observed over $L_s=90-100^\circ$ in Hellas basin (figure 5), when seasonal and latitudinal trends in Hellas O_3 and clouds are at a minimum. However, surface ice is present over regions within Hellas basin at this time.

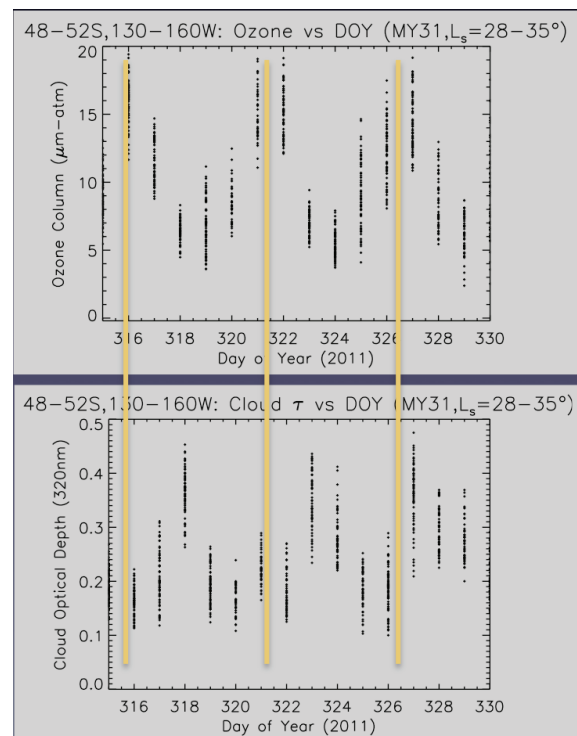


Figure 9. Periodic variations in southern high latitude MARCI O_3 columns (~ 50 S, 145W for southern fall) are compared to coincident cloud optical depth variations².

While the above comparisons of MARCI O₃ observations to LMD GCM O₃ and MARCI cloud optical depth measurements do not rule out heterogeneous reactions on Mars clouds, they do indicate it may be difficult to identify in O₃/cloud column measurements. Furthermore, a detailed comparison of data versus model O₃ and cloud columns has yet to occur. In particular, Mars GCM models (including the LMD GCM) do not accurately simulate Mars cloud columns¹⁵. For example, comparison of the heterogeneous and homogeneous LMD GCM simulations for Hellas basin in figure 5 indicates strong cloud activity beginning well before L_s=50°. By comparison, MARCI cloud optical depths remain very low until L_s=80°.

Conclusions:

The presented MARCI results for Mars column O₃ values represent a preliminary assessment of this new atmospheric data product. These MARCI data combine daily global mapping over ~4 MY with a quantitative column measurement uniquely sensitive to low water vapor conditions (high latitudes, Hellas) during cold seasons (fall-winter-spring, aphelion). They are also accompanied by quantitative cloud optical depth measurements, except over surface-ice⁵. MARCI O₃ data provide a new data set for investigation of Mars polar dynamics with uniquely resolving spatial/temporal coverages. Mars O₃ columns are very sensitive to variations in water vapor/temperature over low water vapor atmospheric (≤ 1 pr- μ m) regions. Polar vortex wave activity is very directly reflected in MARCI O₃ polar maps.

Hellas basin presents less dramatic fall-winter-spring O₃ increases than do the polar regions. But it clearly exhibits both similar and distinctive seasonal variations, indicative of a distinct atmospheric environment on Mars. MARCI daily mapping O₃ and cloud measurements provide a new window into this environment. They also support unique sensitivity to potential heterogeneous chemistry on Mars cloud particles. A preliminary assessment does not indicate a strong observable signature from such chemistry, relative to current data and models comparisons. However, detailed model-data comparisons (including cloud optical depths, which the models do not simulate well) are required to assign limits on the specificity of MARCI O₃ measurements to heterogeneous chemistry. Finally, we note the significant potential for this distinctive global data set in defining new aspects of Mars inter-annual variability.

We encourage the Mars atmospheric science community to work with MARCI cloud and O₃ measurements. The large volume of these data sets presents format challenges. By the time of the meeting, we will be providing subsets of the data in NETCDF and "ddd" formats (along with sample IDL code for reading the latter structure) at:

<https://gemelli.space-science.org/twiki/bin/view/MarsObservations/MarciObservations/OzoneAbundances>

Bibliography:

- (1) Malin et al, Icarus, 194, 2008.
- (2) Clancy et al, DPS BAAS 45, 2013.
- (3) Lefèvre et al, JGR, 109, 2004.
- (4) Lefèvre et al., Nature, 454, 2008.
- (5) Wolff et al., DPS BAAS 42, 2011.
- (6) Perrier et al., JGR, 111, 2006.
- (7) Parkinson and Hunt, JAS, 29, 1972.
- (8) McElroy and Donahue, Science, 177, 1972.
- (9) Barth et al, Science, 179, 1973.
- (10) Clancy and Nair, JGR, 101, 1996.
- (11) Encrenaz et al., A&A, 484, 2008.
- (12) Smith et al, JGR, 114, 2009.
- (13) Encrenaz et al., A&A, 459, 2006.
- (14) Forget, 2nd International Mars conf., 2006.
- (15) Haberle et al, Fall AGU, 2011.